Mapping the Antenna Gain at the RPA

March 20, 2001

G. R. Harp and R. F. Ackermann

Abstract

The gain patterns of some of the RPA antennas are characterized using a two element interference technique. One antenna is given a fixed pointing toward a satellite while a second antenna is swept through its entire range of motion. The signals from these two antennas are cross correlated to provide a 2D map of the gain. This provides a direct measurement of the effective area (4.85 m^2 for RPA6) implying an antenna efficiency of about 48%. We used this technique to measure the amplitude of satellite signals scattered from neighboring antennas into the sidelobes of RPA7. The high-angle sidelobe amplitude was found to vary strongly depending on the position of the other antennas. We conclude that inter-antenna scattering will seriously compromise our ability to form a beam (or null) in the high angle sidelobes at the RPA. An attempt is made to extrapolate these results to the proposed ATA configuration.

Experiment and Analysis

Figure 1 displays a summary of the measurement and analysis. The first antenna is pointed toward a satellite (Solidaridad F2), which has a right-hand circular polarization. The electronics are tuned with a center frequency of 1530.58 MHz and a bandwidth of 10 MHz. (Additional measurements were made with a 150 kHz bandwidth giving essentially identical results.) The second antenna is then swept over its full range of motion. The signals from the "X" polarizations of both antennas were digitally mixed to a complex basis, and then the autocorrelation of antenna 1 (ψ_{11}) and the cross correlation of antennas 1 and 2 ($\tilde{\psi}_{12}$) were calculated.

$$\psi_{11} = \int \left| \tilde{E}_{1x} \right|^2 dt \qquad \text{and}$$

$$\tilde{\psi}_{12}(\Omega_2) = \int \tilde{E}_{1x} \cdot \tilde{E}^*_{2x} \, dt , \qquad \text{where } \Omega_2 = (\vartheta_2, \phi_2)$$

Since the satellite signal is RHCP, we are guaranteed that the two signals will correlate, in spite of the fact that the "X" polarizations of the feeds are not aligned. No attempt was made to compensate for the fact that at large polar angles, ϑ_2, antenna 2's polarization acquires a component perpendicular to the plane of polarization of the satellite signal.

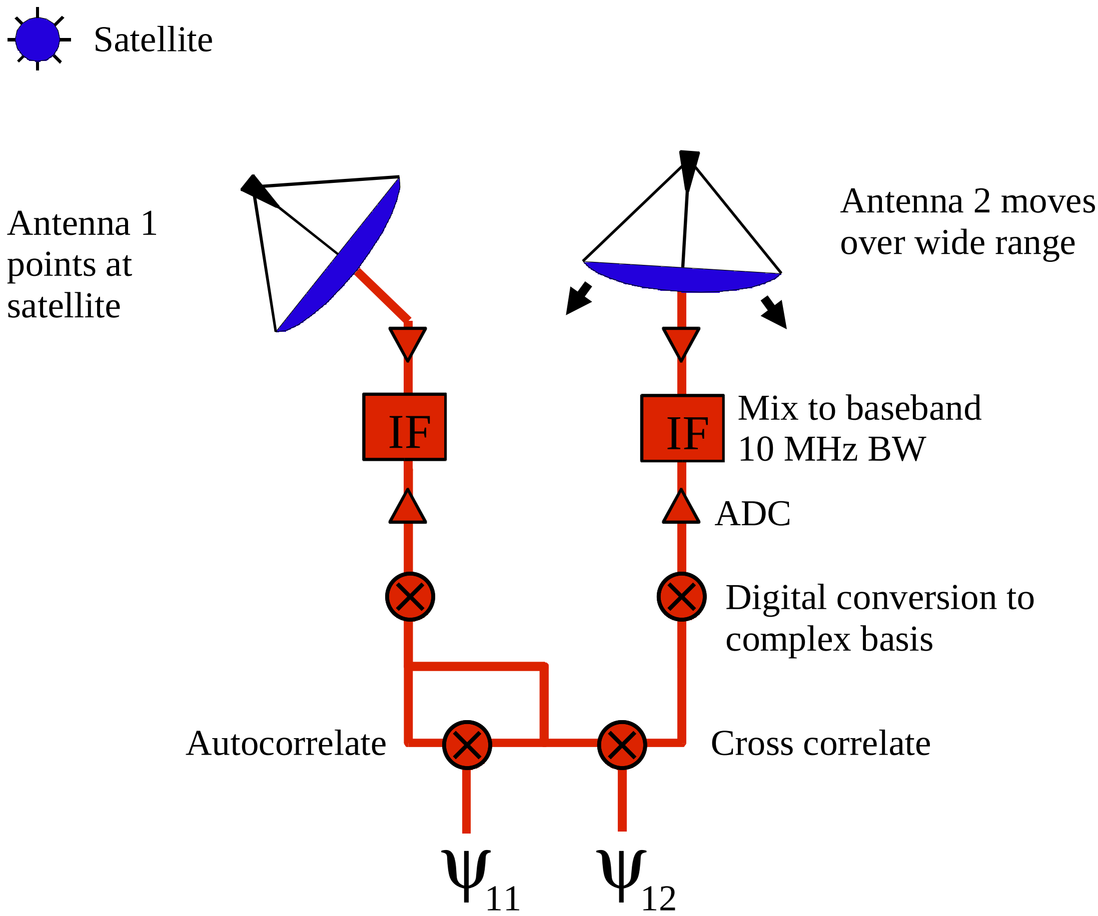

Fig. 1. Block diagram of the experimental measurements.

From ψ_{11} and $\tilde{\psi}_{12}$ we calculate the raw antenna gain, G_r, from

$$G_r(\Omega_2) \quad = \quad \left|\frac{\tilde{\psi}_{12}}{\psi_{11}}\right|^2 .$$

It is important to divide by ψ_{11} in the above equation since the output of the satellite varies with time. The ratio $\tilde{\psi}_{12}/\psi_{11}$ is proportional to the electric field amplitude entering antenna 2 as a function of angle. We square this amplitude to put the figure into units of power. Another analysis would use the amplitude to characterize the dish surface using a process related to holography. This type of analysis will be the subject of a future memo.

Next the raw gain is normalized relative to the gain of an isotropic antenna, $G_{iso} \equiv 1$. Since the integral of G_{iso} over all angles is 4π, this normalization is accomplished by

$$G(\Omega_2) = AG_r(\Omega_2), \qquad \text{where} \qquad A^{-1} = \frac{1}{4\pi}\int_{4\pi} G_r(\Omega_2)\, d\Omega_2 .$$

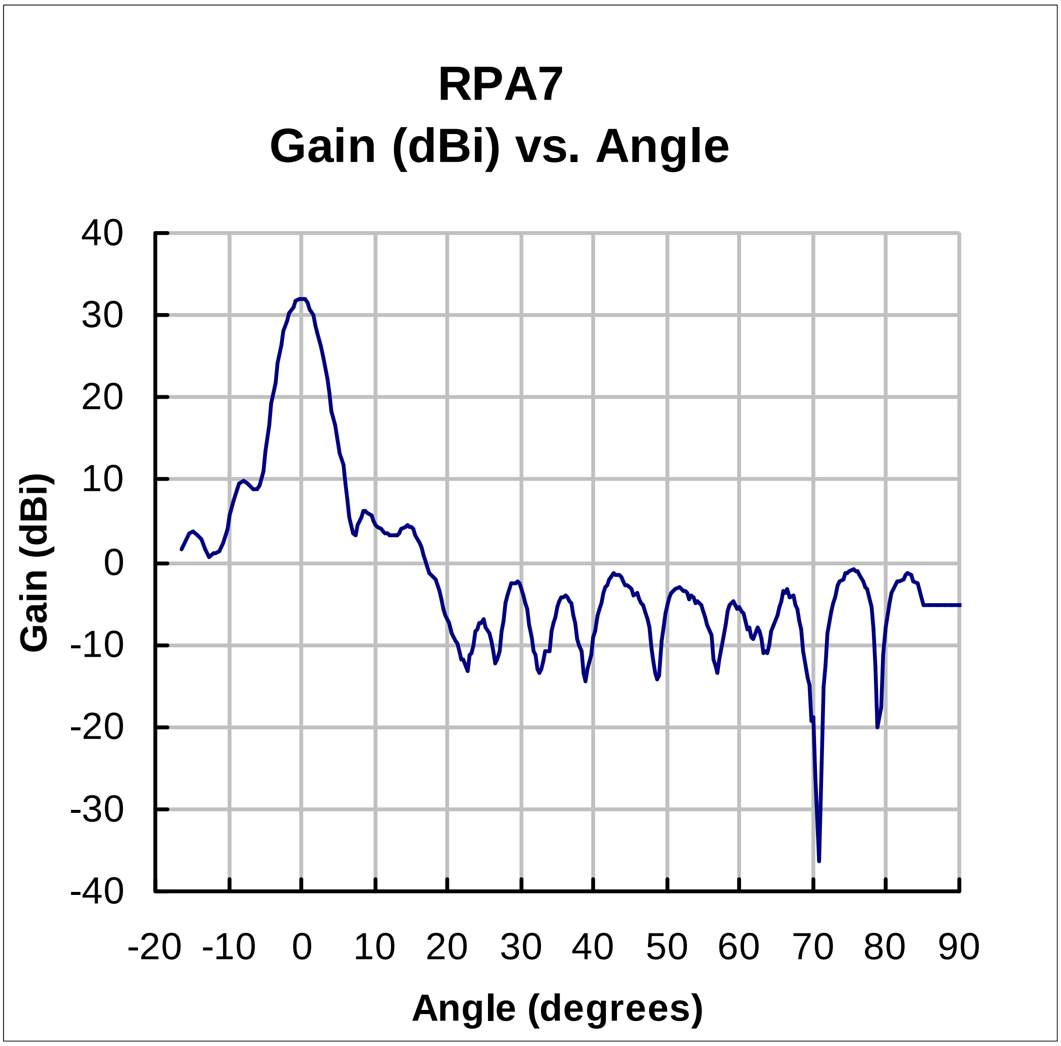

Fig. 2. Plot of the antenna gain vs. polar angle. Polar angle is measured from the direction toward the satellite.

Figure 2 displays line scan through a typical gain spectrum. Because our measurements of G_r do not extend over the entire sphere, we must estimate its value in the areas we cannot measure. To normalize the spectrum in figure 2, we assumed azimuthal symmetry and the average gain over the range $30° < \vartheta_2 < 85°$ was used for the range $85° < \vartheta_2 < 180°$.

Results

In figure 2, the maximum gain is 32 dB, or 1585 times higher than that expected for an isotropic antenna. From this we may calculate the maximum effective area, $A_{e,\max}$, of our antenna from[1]

$$A_{e,\max} = \frac{\lambda^2}{4\pi} G_{\max} = 4.9 \text{ m}^2.$$

This is to be compared with the actual area of the dish (diameter 3.6 m), 10.2 m^2. From these we calculate that the efficiency of this antenna (including the feed, etc.) is about 48%. This is a reasonable number for the present antenna type.

A 2D plot of the gain over the measurable solid angle of RPA6 is displayed in figure 3. This plot is in the "natural" coordinate system of the antenna: the horizontal and vertical scales are linear in the direction cosines, (u , v), where

$u = \cos(\phi)\sin(\vartheta)$, and

$v = \sin(\phi)\sin(\vartheta)$.

and ϑ and ϕ measure zenith angle and azimuthal angle, respectively, in a coordinate system aligned with the ground. The white circle represents the horizon (ϑ = 90°) and the image intensity is proportional to the gain in dBi.

It is convenient to convert to a coordinate system where the center of the image is aligned with the center of the gain pattern (e.g. the direction towards the satellite). This transformation is accomplished as follows. Defining a "z" coordinate, $w = \cos(\vartheta)$, for the data, we have G(u , v , w). We wish to find a coordinate system (u' , v' , w') where zenith, $\hat{w}'$ = (0, 0, 1), is aligned with the direction of peak gain, $\vec{r}_p$. The x- and y-axes, $\hat{u}'$ and $\hat{v}'$, of our primed coordinate system are arbitrary. Expressing $\hat{u}'$, $\hat{v}'$ and $\hat{w}'$ in terms of the unprimed coordinate directions $\hat{u}$, $\hat{v}$, and $\hat{w}$ we choose

$\hat{w}' = \vec{r}_p$,

$\hat{v}' = \dfrac{\hat{w}' \times \hat{w}}{|\hat{w}' \times \hat{w}|}$, and

$\hat{u}' = \hat{v}' \times \hat{w}'$.

[1] See M. L. Meeks in "Methods of Experimental Physics, V. 12 Part B, Astrophysics – Radio Telescopes," ed. by M. L. Meeks, Academic Press, p. 3 (1976).

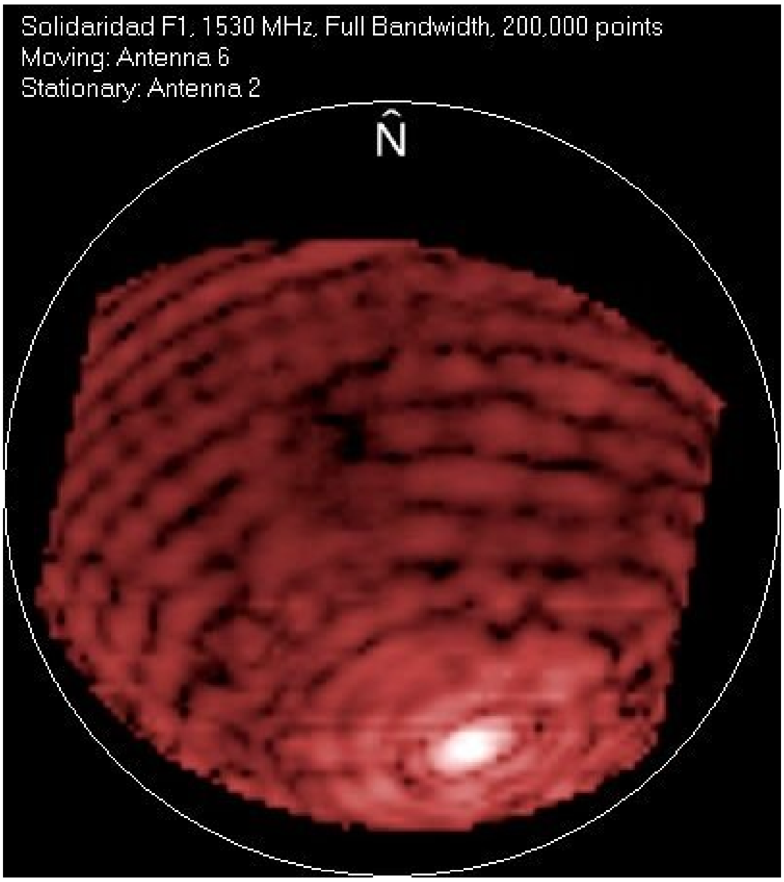

Fig. 3. Two dimensional plot of the antenna gain. To understand this image, imagine you are looking down onto the surface of a sphere. The white circle represents the horizon. The intensity is plotted on a log scale, and the bright spot appears where the moving antenna is pointed directly at the satellite. Notice that the range of motion for this antenna is tilted slightly toward the southerly direction.

For any $\vec{r}$, we can calculate $\vec{r}\,'$ from

$u' = \vec{r} \cdot \hat{u}'$,

$v' = \vec{r} \cdot \hat{v}'$, and

$w' = \vec{r} \cdot \hat{w}'$.

The gain of figure 3 was transformed in this way and plotted in figure 4. Note that the rings around the main peak are now circular, as expected for this coordinate system. The same transformation was applied to the data in figure 2 before plotting.

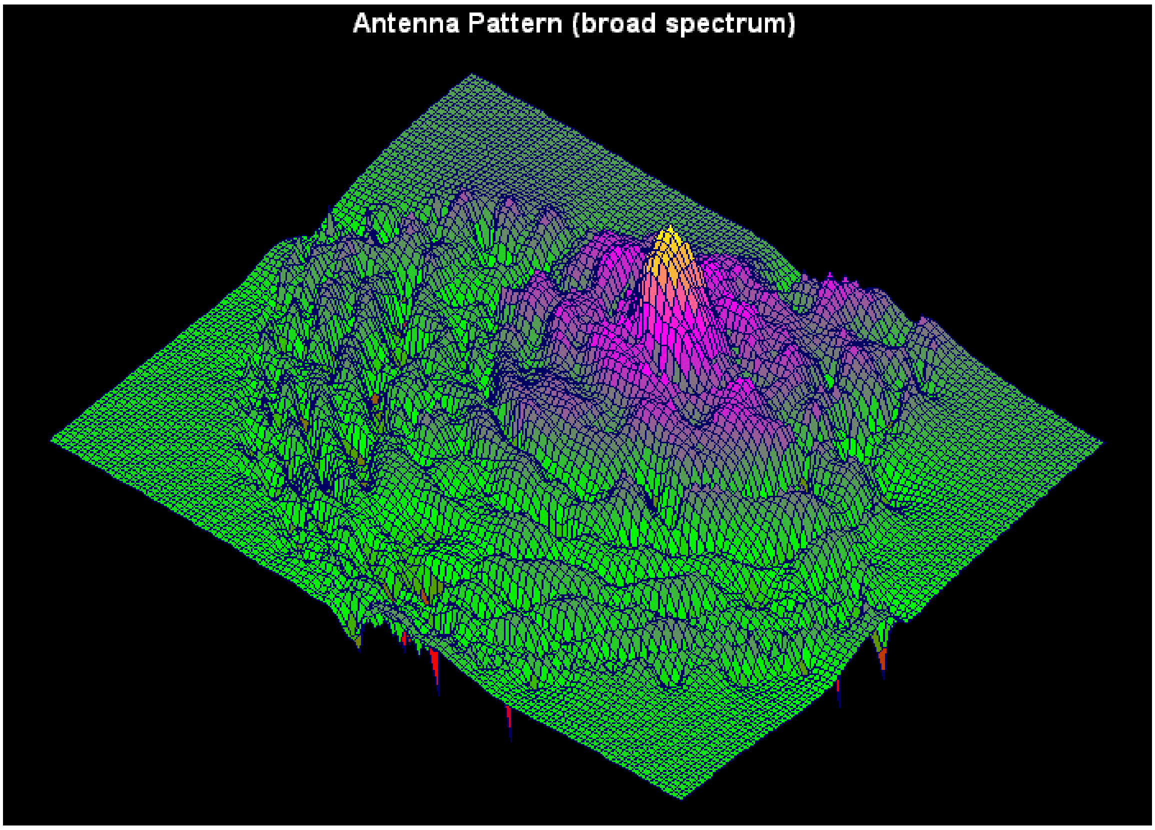

Fig. 4. Gain pattern of fig. 3 after transformation to a coordinate system centered on the beam peak. Again, the vertical scale is logarithmic in antenna gain.

Inter-Antenna Scattering into Pattern Side Lobes

When the RPA antennas are pointed at low elevation, they often obstruct one another's view because they are packed tightly together. In this situation, the antenna of interest is viewing the backside of its neighbor, assuming they are both pointed in the same direction. The backside of a dish makes a pretty good convex mirror, so for some geometries our antenna will see a demagnified image of the rearward sky (and ground) in this mirror. We wish to determine the magnitude of such inter-antenna scattering.

We made nominally identical measurements of the gain on RPA7 (the central antenna) where the only changing variable was the positions of RPA2-RPA6 (RPA1 always pointed toward the satellite). Line scans were acquired as depicted in figure 5, along a path that passed through the pattern maximum on the south side, and very close to the direction of RPA6 on the north side.

Figure 6 shows two such line scans, one taken with the antennas in "open flower" arrangement (antennas pointing away from RPA7 as in figure 5), and another in the "closed flower" arrangement (antennas pointing toward RPA7 to maximize its unobstructed view). The curves of figure 6 show significant differences, well above the random variations we observe for successive identical scans.

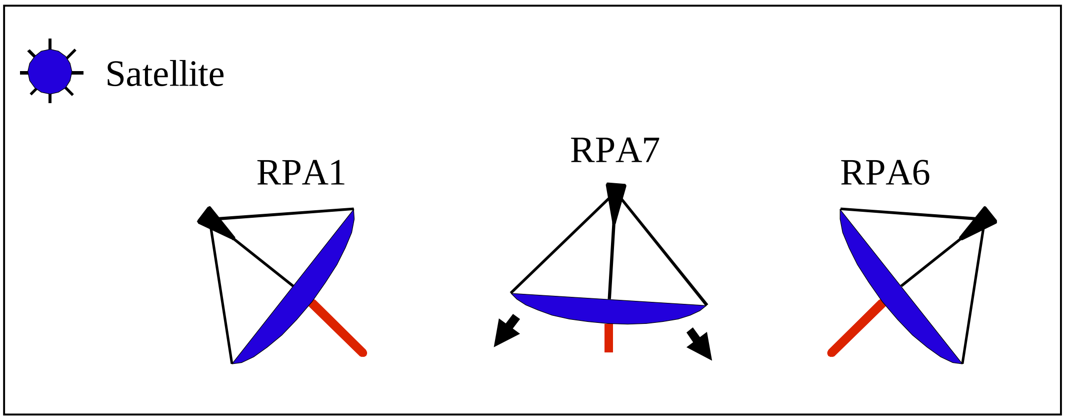

Fig. 5. Geometry of the “open flower” line scan in figure 6.

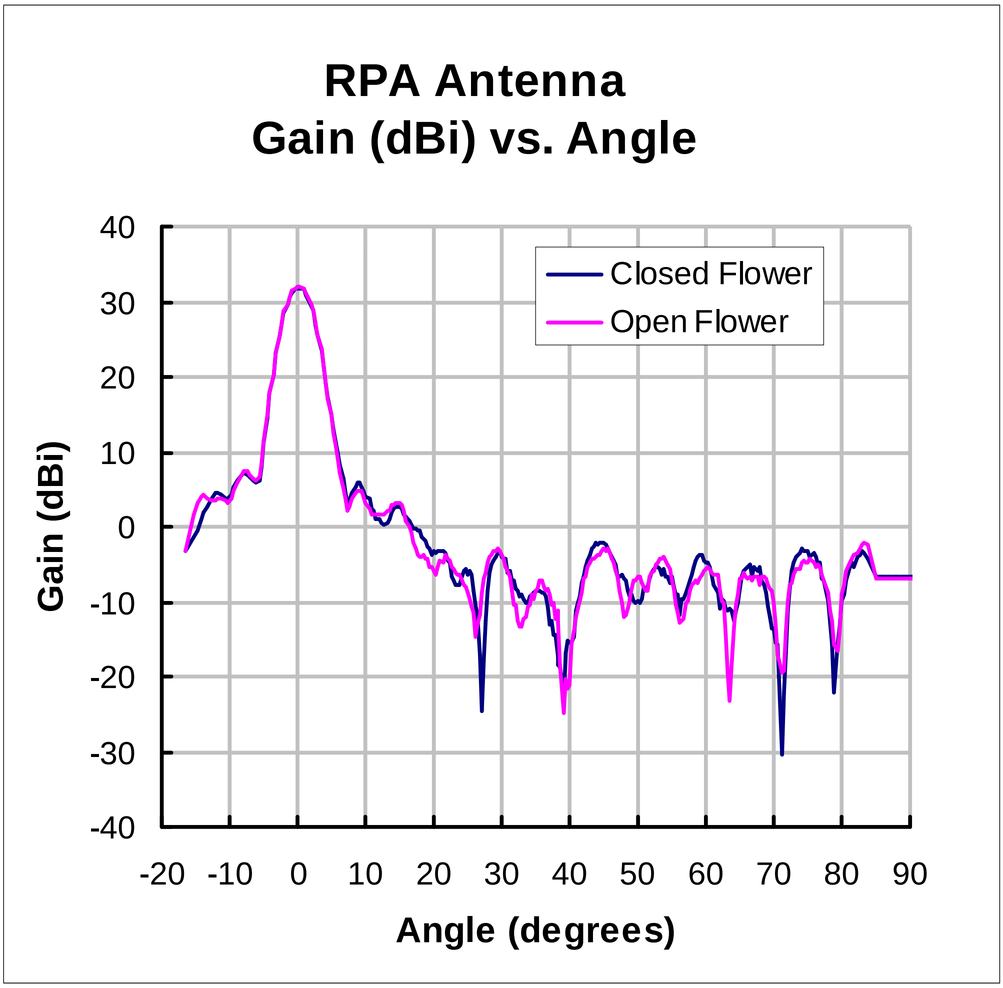

Fig. 6. Two nominally identical line scans where RPA1 is fixed in the direction of the satellite and RPA7 moves through its range of motion. The only difference between the two scans was the position of the other, uninvolved antennas.

To more easily gauge the magnitude of these changes, another type of scan was performed where RPA7 was held in fixed position near zenith while another "uninvolved" antenna was moved. Figure 7 shows one such scan. Here, RPA6 was set at a constant elevation angle of 50° and rotated about the zenith axis (azimuth). The measurement was repeated twice and the two plots are superimposed. We plot the normalized gain, defined as G_r / G_{peak}, where G_{peak} is the gain in the direction of the satellite. The zero of azimuthal angle corresponds to the value where RPA6 is pointed towards the satellite.

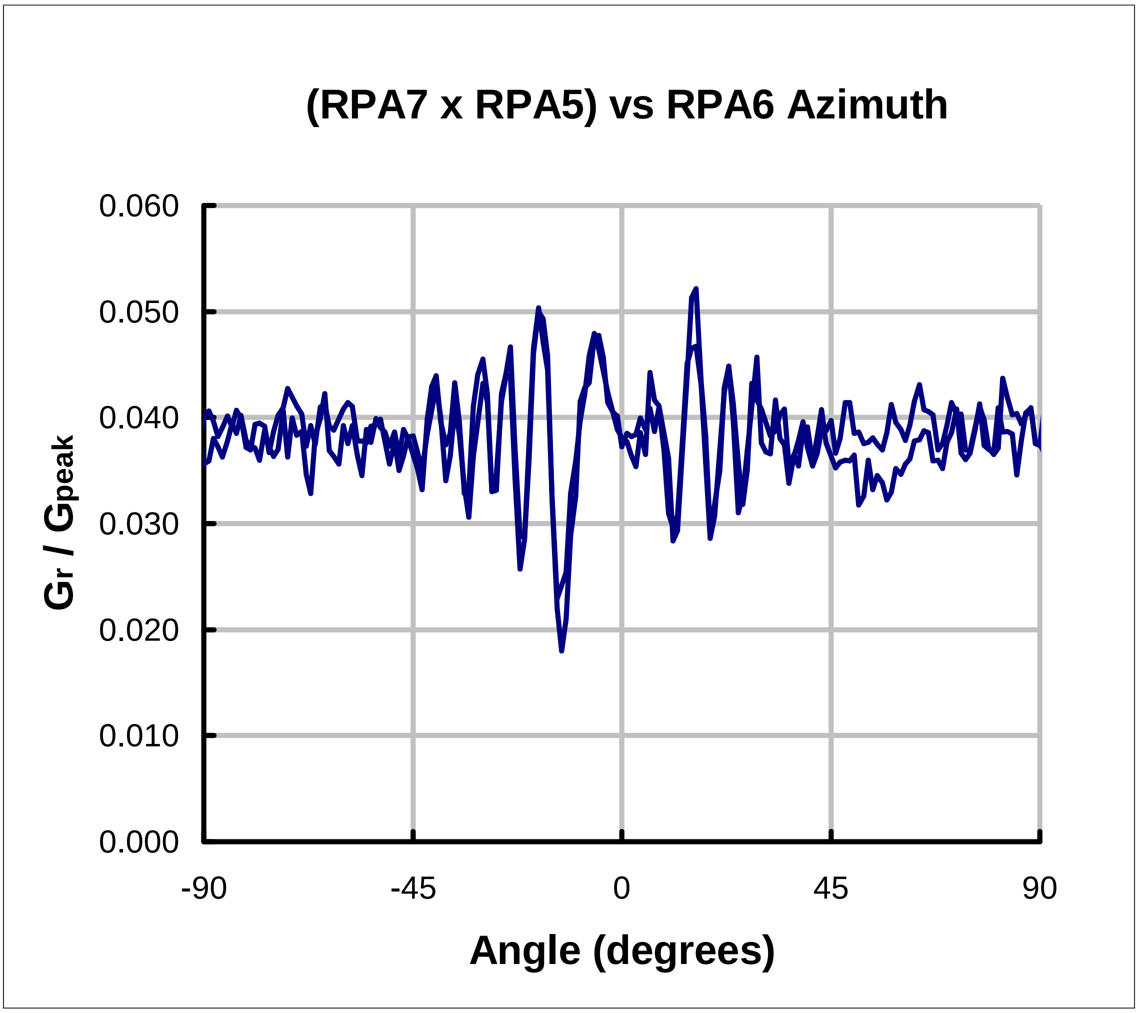

Fig. 7. Plot of G_r / G_{peak} for RPA7, which is held in fixed position. The gain is plotted as a function of the azimuthal position of RPA6. The strong variations near 0° are well above the random noise variations, and have an amplitude of a few percent of the gain in the main beam.

The gain of RPA7 has substantial variation depending on the position of RPA6. To our surprise, the maximal variation occurred not when the backside of RPA6 was directed at RPA7, but when RPA6 was pointed towards the satellite. We believe this happens because RPA6 focuses the satellite signal upon its own feed, which absorbs only a fraction of the signal projected onto it. The rest of the signal is scattered. Indeed, the maximal excursions of G_r occur when RPA6 is pointed about 10° away from the satellite, at which time the signal is focused onto the choke ring on RPA6, which strongly scatters the signal.

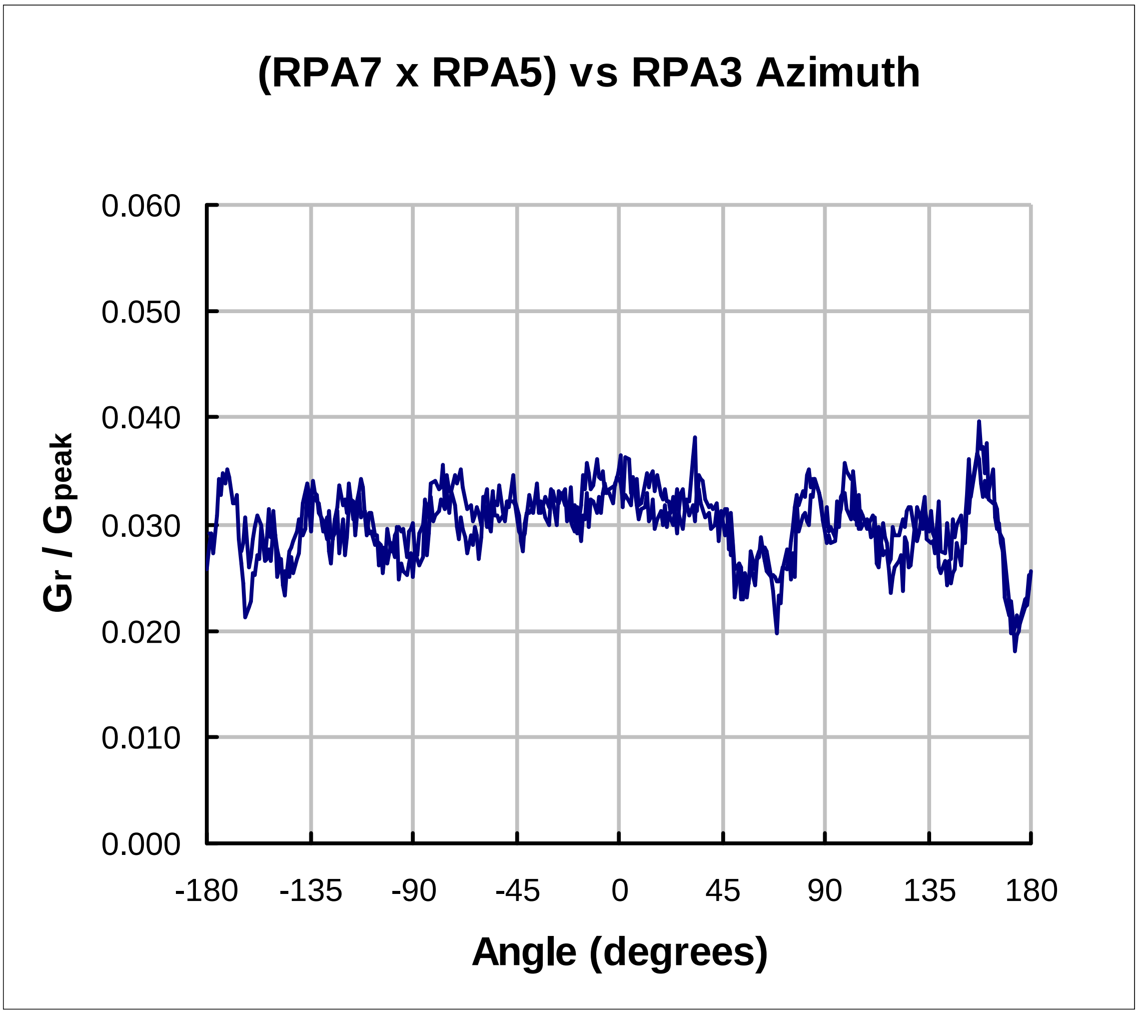

Fig. 8. Scan similar to that of fig. 7 except that here RPA3 is rotated instead of RPA6.

Several other scans, similar to figure 7 were studied. For example, figure 8 shows the result of spinning RPA3 instead of RPA6. RPA3 is "in front of" RPA7 (i.e. closer to the satellite), as compared with RPA6 which is "behind" RPA7. Again we observe substantial variations in gain, but the peak variations occur near 180°. In this case RPA3's dish blocks the line of sight between RPA7 and the feed of RPA3 at azimuth = 0°. It isn't obvious what part of RPA3 acts as the scatterer in this case, but reproducible gain variations are clearly observed. This figure demonstrates that inter-antenna scattering can be significant even when the "uninvolved" antennas do not point at the RFI source.

Discussion

Figures 7 and 8 have important implications for certain methods of RFI mitigation that have been proposed at the RPA. In particular, beam forming (or beam nulling) in the high-angle sidelobes will be very inaccurate, unless inter-antenna scattering is explicitly taken into account. The gain for each antenna depends on the positions of all the other antennas in the array. Evidently the scattering (and gain) will change drastically depending on the position of the satellite in the sky, $(\vartheta_{Sat}, \phi_{Sat})$. In general, $G = G(\vartheta_2, \phi_2, \vartheta_{Sat}, \phi_{Sat}, \vartheta_1, \phi_1, \vartheta_3, \phi_3, \cdots)$. To completely specify the antenna gain at the RPA, we must measure all these dependencies, which is impossible.

However, we don't really need all these dependencies since in most measurements the antennas move together. Applying this constraint makes the problem simpler, but the gain still depends on the satellite position: $G = G(\vartheta_2, \phi_2, \vartheta_{Sat}, \phi_{Sat})$. For a reasonable point density at the RPA (100 points in u and v), we must measure the gain pattern at 10^8 points. Given the difficulty of making measurements as a function of satellite position, this too is probably impossible.

If instead, we approximate G by $G = G(\vartheta_2, \phi_2)$, figure 7 indicates our gain will be in error by roughly 50%. When forming a beam (or null) in the high-angle sidelobes, we can expect these errors to cancel out on average, so with 7 antennas the beam phase / amplitude error will be in the range of 10-20%. This might be adequate for some crude experiments, but it is not promising for meaningful testing of satellite nulling methods at the RPA.

Another question is how the scattered satellite amplitude is entering into RPA7. Initially we guessed that it was bouncing off of RPA7's dish and entering the feed in the "normal" way. However, figure 7 indicates that most of the scattered signal is entering RPA7 via the feed spillover across the edge of the dish. In figure 7, RPA7 was actually pointed 5° *away* from RPA6, in the direction of the satellite. (This direction was chosen to make measurements at a local maximum of G_r.) Based on this and other measurements, we now believe that feed spillover is the primary pathway for scattering to enter RPA7.

As a final point, we raise the question of how inter-antenna scattering might affect beam forming in the **primary beam** at the RPA. We leave this question open for future research.

Extrapolation of Results to the ATA

In this section we attempt to extrapolate the above results to the ATA. First we note that even 2D measurements of $G = G(\vartheta_2, \phi_2)$ will be a challenge. Because the ATA antennas have twice the diameter of the RPA antennas, we must measure and store a grid of 400 x 400 points for the gain at 1 GHz. At 10 GHz, the grid grows to 4000 x 4000.

Furthermore, each gain pattern has validity over a frequency range of only ~50 MHz,[2] so we may have to repeat these measurements 200 times for all 350 antennas in the array. This gives a daunting total of 10^{11} individual measurements. In practice, we may need the gain only at selected frequencies, so this number could be reduced. However, a complete measurement of $G = G(\vartheta_2, \phi_2, \vartheta_{Sat}, \phi_{Sat})$ would require 10^{22} measurements, which is clearly out of the question.

To estimate the scattering magnitude at the ATA, consider that the distance of closest approach between antennas is about two antenna diameters – the same as at the RPA. However, the packing density at the ATA will be much lower, which should reduce scattering overall. We optimistically estimate that instead of 50%, we may see 5% changes in G caused by inter-antenna scattering at the ATA (in the high angle sidelobes).[3]

Using this estimate and 350 antenna, we predict beam amplitude / phase errors of order 0.3% when forming beams in high angle sidelobes. To consider a specific example, this implies a maximum of 25 dB reduction in unwanted field, or 50 dB reduction in unwanted power, when forming a sidelobe null on a satellite at the ATA. Even for Iridium, this is probably sufficient suppression for most astronomical observations. However, in the vicinity of satellite carrier tones, beam nulling will probably not provide sufficient signal suppression for the narrow band observations performed in the SETI search.

Conclusions

We have mapped the gain pattern of some of the RPA antennas using a two element interference technique. These measurements indicate a collection efficiency of about 50% for the RPA antennas. We have also discovered that there is significant inter-antenna scattering due to the close-packed configuration of the RPA. This inter-antenna scattering will make sidelobe beam forming rather inaccurate at the RPA. From these measurements, we crudely estimate the inter-antenna scattering in the proposed ATA configuration. For the ATA, we find that sidelobe beam forming will be reasonably accurate in the presence of inter-antenna scattering, with a phase / amplitude error of about 0.3% caused by scattering.

---

[2] An easy way to estimate this is to ask, "How large a change in frequency is required to put two waves out of phase by 180° while they traverse the dish radius?" The answer is, $\Delta f = c / D$, where c is the speed of light and D is the dish diameter.

[3] The question of feed spillover at the ATA is interesting. At the ATA, the feed points away from the primary reflector, and the majority of the spillover occurs at the edge of the secondary, which is projected onto the sky. This should reduce the amplitude of scattering pathways into the antenna when it is pointed at zenith, though they are enhanced at low elevation. Since most observations are performed at higher elevation, this is probably an advantage.